Indian Journal of Chemistry
Vol. 56A, August 2017, pp. 805-813

Vitamin-B6 Schiff base dioxovanadium(V) complex for targeted visible light-induced anticancer activity

Arun Kumar, Samya Banerjee, Sanjoy Mukherjee & Akhil R Chakravarty*

Department of Inorganic and Physical Chemistry, Indian Institute of Science, Sir C V Raman Avenue, Bangalore 560 012, India
Email: arc@ipc.iisc.ernet.in

Received 23 May 2017; revised and accepted 24 July 2017

A dioxovanadium(V) complex of vitamin-B6 Schiff base [VO_2L] (**1**) (where H_2L·HCl is 3-hydroxy-5-(hydroxymethyl)-4-(((2-hydroxyphenyl)imino)methyl)-2-methylpyridin-1-ium chloride) has been prepared and structurally characterized. Its photo-induced cytotoxicity and mechanism of cell death has been studied. Single crystal X-ray structure shows five-coordinate square-pyramidal geometry of the complex having the dianionic O,N,O-donor tridentate vitamin-B6 Schiff base and two *cis*-oriented oxo ligands bound to V(V). DFT study shows the HOMO located on the amino-phenolic moiety, while the LUMO is on the protonated aromatic unit, i.e., the pyridiniumphenolate moiety. Vitamin-B6 transporting membrane carrier (VTC) pathway seems to be responsible for the higher cellular uptake and activity of the complex into the cervical HeLa and breast cancer MCF-7 cells in preference to the normal embryonic fibroblast 3T3 cells. The complex exhibits reactive oxygen species (ROS) mediated apoptotic photocytotoxicity in visible light of 400–700 nm in the cancer cells (IC_{50}: ~16 μ*M*), while being essentially non-toxic in the dark. Alkaline Comet assay shows damage of the nuclear DNA.

Keywords: Bioinorganic chemistry, Photocytotoxicity, Crystal structure, Cell apoptosis, Schiff base, Vitamin-B6 Schiff base, Vanadium

Photodynamic therapy (PDT) has emerged as a new treatment modality for cancer[1-11]. PDT being selective, damages only the photo-irradiated cancer cells with minimal effect to the unexposed normal cells. The FDA approved PDT drug is Photofrin® which on red light activation (632 nm) produces singlet oxygen ($^1O_2$) as the reactive oxygen species (ROS)[12-14]. Selective activation of Photofrin® at the tumour site circumvents the side effects associated with the widely used platinum(II) based chemotherapeutic drugs[1,2,12-14]. Photofrin®, however, suffers from several limitations: (i) causing hepatotoxicity due to its oxidative degradation to bilirubin, (ii) skin photosensitivity for a long period due to significant localization on the skin tissues and (iii) low selectivity towards cancer cells over normal ones[1,2,4,5,15]. Recent reports have shown that photoactive transition metal complexes could be the potential alternatives to this drug[16-30]. The current focus in this chemistry is to develop tumour targeting photoactive anticancer metal complexes that can recognize the intrinsic differences between the cancerous and healthy cells and thus minimize the drug related side effects[31,32]. The photoactive complexes bearing a tumour recognition moiety is expected to improve the selectivity[33,34]. We have previously shown that vitamin-B6 (VB6) conjugated metal complexes specifically localize in the tumour cells over their normal counterpart[35-37]. Vitamin-B6 is known for its biological importance, involved in a variety of metabolic and physiological processes such as lipid, glucose and amino acid metabolisms[38-40]. It is an important cofactor in DNA biosynthesis, hence has an important role in cellular growth and also is a protective factor against various cancers. VB6 derivatives are known to inhibit tumorigenesis[41]. Cellular uptake of VB6 is through its transporting membrane carrier (VTC) mediated diffusion[42,43]. Since rapidly growing tumour cells demands high dosage of VB6 for their survival, the VB6 incorporated metal complexes are prone to achieve VTC mediated preferential uptake into the cancer cells over the normal ones[35-37]. The present report is based on our work on the anticancer potential of a new ternary dioxovanadium(V) complex [VO_2L] having a VB6 incorporated Schiff base moiety. Vanadium being useful trace element in the biological systems, its compounds are used as insulin mimetics and antitumor agents as well[44-46]. While oxovanadium(IV) complexes are known for their photo-induced anticancer activity, dioxovanadium(V) complexes showing similar activity remain virtually unexplored[9-11,20,21].

Besides, the reported dioxovanadium(V) complexes show UV-light induced cytotoxicity which is not preferred in PDT[47,48].

Herein, we present the synthesis, characterization, tumour selective visible light-induced anticancer activity of a new dioxovanadium(V) complex [VO_2L] (**1**), where $H_2L{\cdot}HCl$ is 3-hydroxy-5-(hydroxymethyl)-4-(((2-hydroxyphenyl)imino)-methyl)-2-methylpyridin-1-ium chloride (Fig. 1). The complex has been structurally characterized by X-ray crystallography. Significant results of this report include: (i) VTC-mediated uptake of the complex into the cancer cells, (ii) apoptotic photo-cytotoxicity in HeLa and MCF-7 cancer cells (IC_{50} < 20 μM) in visible light of 400-700 nm while remaining less toxic in 3T3 normal cells and in dark, and, (iii) the photo-activated apoptotic cell death resulting from damage to nuclear DNA from oxidative cell stress due to generation of intracellular ROS on photo-activation.

Materials and Methods

The reagents and chemicals were procured from commercial sources (Sigma-Aldrich, USA) and used as such without any further purification. $VO(acac)_2$ (Hacac, acetylacetone) and pyridoxal hydrochloride were purchased from Sigma-Aldrich. Solvents were purified following standard literature procedures[49]. Agarose (molecular biology grade), 2,7-dichloro-fluoresceindiacetate (DCFDA), propidium iodide (PI), 3-(4,5-dimethylthiazol-2-yl)-2,5-diphenyltetrazolium bromide (MTT), Dulbecco's modified eagle medium (DMEM), and fetal bovine serum (FBS) were obtained from Sigma (USA). OxiSelect™ Comet assay kit was purchased from Cell Biolabs Inc. The Schiff base ($H_2L{\cdot}HCl$) was prepared following a literature report by reacting pyridoxal hydrochloride with 2-aminophenol in dry methanol at room temperature[50].

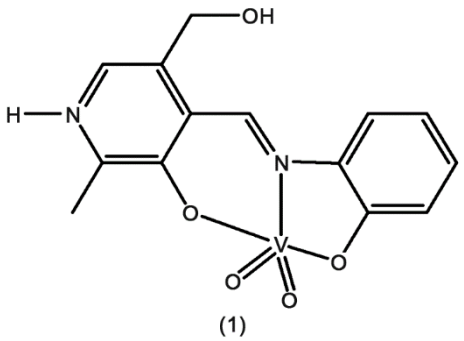

(1)

Fig. 1 — Structure of the dioxovanadium(V) [VO_2L](**1**) and the vitamin-B6 Schiff base complex.

Elemental analysis was done by a VarioELcube CHNS Elemental analyzer. The solid state IR and UV-visible spectra were recorded using Bruker Alpha and Perkin-Elmer Spectrum 650 spectrophotometers, respectively, at 25 °C. Electrospray ionization (ESI) mass spectral measurements were made using Agilent 6538 Ultra High Definition (UHD) accurate Mass-Q-TOF (LC-HRMS) and Bruker Daltonics make Esquire 300 Plus ESI mass spectrometers. NMR spectra were recorded on a Bruker Avance 400 NMR spectrometer (400 MHz). Flow cytometric analysis was done using FACS Calibur (Becton Dickinson cell analyser) at FL1 channel (595 nm). Fluorescence microscopic experiments were performed by Apotome.2 fluorescence microscope using an oil immersion lens of 63X magnification.

Synthesis of the complex

Complex **1** of the formulation [VO_2L] was prepared by reacting an ethanol solution of $VO(acac)_2$ (0.265 g, 1.0 mmol in 4 mL ethanol) to a hot ethanol solution of $H_2L{\cdot}HCl$ (0.295 g, 1.0 mmol in 10 mL methanol). The solution colour changed from light red to deep red. After refluxing for 2 h, the solution was cooled to room temperature to obtain a red precipitate of the complex. The precipitate was isolated and washed with ethanol, chilled methanol, chloroform and finally dried over P_4O_{10} under vacuum.

Yield = 77%. Anal. (%): Calc. for $C_{14}H_{13}N_2O_5V$ (**1**): C, 49.43; H, 3.85; N, 8.23. Found: C, 49.79; H, 4.06; N, 8.11. ESI-MS in MeOH: m/z 614.1125 $[M+H]^+$. IR data cm^{-1}: 1610 s (C=N), 1586 m, 1487 w, 1377 m, 1266 s, 1155 m, 968 s (V=O), 810 m, 540 m, 462 m (s, strong; m, medium; w, weak). UV-visible in DMF [λ_{max}/nm (ε/M^{-1} cm^{-1})]: 465 (23700), 290 (74200). Molar conductivity in DMF at 298 K [Λ_M/S m^2 M^{-1}]: 12.

X-ray crystallographic studies

Crystals of complex **1**·MeOH were grown via slow evaporation of a methanolic solution of the complex over four days. A crystal of 0.44×0.4×0.2 mm^3 size was mounted on a glass fibre with epoxy cement. All geometric and intensity data were collected at room temperature using an automated Bruker Smart Apex CCD diffractometer equipped with a fine focus 1.75 kW sealed tube Mo-K_α X-ray source (λ = 0.71073 Å) with increasing ω (width of 0.3° per frame) at a scan speed of 5 sec per frame. Intensity data were collected using ω-2θ scan mode and due corrections were made for the Lorentz–polarization effects and for absorption[51]. Patterson and Fourier techniques were used to solve the structure and refinement was

done by full matrix least squares method using SHELXL-2013 present in the WinGx programs (ver. 1.63.04a)[52,53]. The hydrogen atoms of the complex were placed in their calculated positions and refined in the riding mode. The hydrogen atom attached to the pyridoxal nitrogen atom was located in the difference Fourier map. The final refinement included atomic positions for all the atoms, anisotropic thermal parameters for all the non-hydrogen atoms and isotropic thermal parameters for all the hydrogen atoms. Perspective view of the complex was obtained by ORTEP[54]. Crystallographic data and the structure refinement parameters for the complex are given in Table 1.

Table 1 — Selected crystallographic data and structure refinement parameters for complex **1**·MeOH

Emp. formula	C_{15} H_{17} N_2 O_6 V
Formula wt. (g mol^{-1})	372.25
Crystal system	Monoclinic
Space group	*P* $2_1/c$
a (Å)	7.5141(6)
b (Å)	14.1457(11)
c (Å)	14.4731(11)
$\alpha = \gamma$ (°)	90
β (°)	94.078(3)°
V ($Å^3$)	1534.5(2)
Z	4
T (K)	296(2)
ρ_{calc}(g cm^{-3})	1.611
λ (Å) (Mo-K_α)	0.71073
μ (mm^{-1})	0.682
Data/restraints/parameters	4692/ 0/ 285
F(000)	768
Crystal size	0.44×0.40×0.20 mm^3
θ (data collection)	2.718 to 30.646°
Limiting indices	$-10 \le h <= 10$, $-20 \le k <= 20$, $-19 \le l <= 20$
Reflections collected	32749
Ind. reflections	4742 [R(int) = 0.0462]
Completeness to θ = 25.242°	99.8%
Max. and min. transmission	0.869 and 0.741
Goodness-of-fit on F^2	0.903
Final R indices [I > 2σ(I)]	R1 = 0.0314, wR2 = 0.0857
R indices (all data)	R1 = 0.0385, wR2 = 0.0921
Largest diff. peak and hole (e $Å^{-3}$)	0.490 and –0.261

Cell viability (MTT) assay

Approximately 1.0×10^4 HeLa cervical cancer, MCF-7 breast cancer and 3T3 embryonic fibroblast normal cells were plated in each well of a 96-well cell culture plate in DMEM cell culture medium supplemented with 10% fetal bovine serum (10% DMEM) and cultured for 12 h. The assay was performed based upon standard protocols[9-11,17-19,23-25]. The complex was dissolved in DMSO-10% DMEM (1:99 *v/v*) and was added to the cells at various concentrations. Incubation was done for 4 h in the dark with subsequent photo-irradiation for 1 h in phosphate buffer saline (PBS) under visible light of 400-700 nm using Luzchem Photoreactor (model LZC-1, Ontario, Canada) assembled with Sylvania make 8 white fluorescent tubes giving an overall fluence rate of 2.4 mW cm^{-2} (total dose of 10 J cm^{-2}). PBS was replaced with 10% DMEM after photo exposure. Incubation was continued in the dark for further 20 h. A 25 μL of 5 mg mL^{-1} of MTT was added to each well and incubated for 3 h. The culture medium was discarded and 100 μL of DMSO was added to dissolve the formazan crystals. The intensity of formazan was estimated from its absorbance at 540 nm in DMSO using an ELISA microplate reader (BioRad, Hercules, CA, USA). The IC_{50} values were determined using nonlinear regression analysis method by plotting "log(inhibitor) vs. normalized response (variable slope)" using GraphPad Prism version 5.1[55]. To ascertain that the VTC mediated diffusion pathway was responsible for the cellular uptake of the complex, HeLa cells were first incubated with 4 m*M* vitamin-B6 for 45 min with subsequent addition of the complex for the MTT assay following a similar protocol as described above.

DCFDA assay for ROS

DCFDA assay was carried out to detect any generation of intracellular reactive oxygen species (ROS) by the complex upon visible light (400-700 nm) irradiation. HeLa cells were incubated with 20 μ*M* of the complex for 4 h followed by photo-exposure to visible light for 1 h in phosphate buffer saline (PBS). Cells were then harvested by trypsinization and single cell suspension of 1.0×10^6 cells per mL was prepared. The suspension was then treated with 10 μ*M* DCFDA (in DMSO) and kept in the dark for 10 min at 25 °C. Flow cytometric analysis was performed to obtain the distribution of the cells stained with DCFDA[56].

Annexin-V/PI binding assay

To ascertain the pathway of photo-induced cell death by complex **1**, approximately 4.0×10^5 HeLa cells per mL were incubated with the complex (20 μ*M*)

in 10% DMEM for 4 h in the dark, followed by exposure to visible light (400-700 nm, dose 10 J cm^{-2}) for 1 h. The cells were then cultured for 18 h in complete medium under darkness, harvested and washed twice with chilled PBS. The cells were re-suspended in 100 μ*L* Annexin-V binding buffer (100 mmol HEPES/ NaOH, pH 7.4 containing 140 mmol NaCl and 2.5 mmol $CaCl_2$), stained with Annexin-V FITC and propidium iodide (PI), and incubated for 15 min at 25 °C in the dark. A 400 μ*L* of binding buffer was added to the cells after incubation and analysed immediately by flow cytometry[57].

Comet assay

To detect the photo-induced DNA damaging ability of the complex at the single cell level, comet assay was performed. Around 1.5×10^4 HeLa cells were incubated with 30 μ*M* of the complex for 4h in the dark followed by 1h of light irradiation (visible light of 400-700 nm). Cells were subsequently harvested and re-suspended in 75 μL of 0.5% low melting point agarose. The cell suspension was spread over agarose coated microscopic slides and allowed to dry. Successively, the slides were put into cold lysis solution (2.5 *M* sodium chloride, 100 mmol EDTA, 10 mmol Tris-HCl, pH = 10, 1% Triton X100, 10% DMSO) at 4°C for 3 h. After lysis, slides were kept in electrophoresis buffer (300 mmol NaOH and 1 mmol EDTA, pH = 13) at 4 °C. They were incubated for 30 min in the buffer for DNA unwinding followed by electrophoresis in the same buffer at 25 V, 300 mA, 4 °C for 45 min. Slides were neutralized in 0.4 *M* Tris-HCl (pH = 7.5) and stained with Vista Green DNA Dye for 15 min. Images were acquired using Apotome.2 fluorescence microscope (Carl Zeiss, Germany) using a FITC (Fluorescein IsothioCyanate) filter[20,21].

Results and Discussion

Synthesis and general aspects

The complex was prepared from the reaction of vitamin-B6 Schiff base ($H_2L{\cdot}HCl$) with $VO(acac)_2$ in MeOH. The complex was characterized from the spectral and analytical data. ESI-MS spectrum of the diamagnetic complex in MeOH gave a single peak at m/z value of 341.1939 corresponding to $[M+H]^+$. The complex in DMF displayed a broad band near 465 nm assignable to $PhO^- \rightarrow V(V)$ ligand-to-metal charge transfer (LMCT) transition (Fig. 2)[58]. The band near 290 nm was assigned to the ligand-based $\pi\rightarrow\pi^*$ transition[59]. The solid state FT-IR spectra displayed

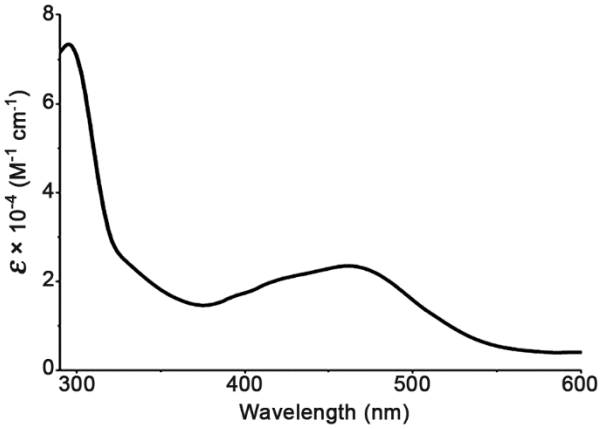

Fig. 2 — Absorption spectrum of complex **1** in DMF.

characteristic IR peaks at 968 cm^{-1} and 1614 cm^{-1} for the V=O and the co-ordinated C=N stretching vibrations, respectively. Molar conductance value of ~12 S m^2 M^{-1} in DMF suggests the non-electrolytic nature of the complex[60,61]. The complex showed good solubility in DMSO, DMF, MeCN and MeOH; moderate solubility in ethanol, water and poor solubility in hydrocarbons. The complex was stable in both solid and solution phases. The complex is redox active showing cyclic voltammetric responses involving the metal center and the ligands in 20% aqueous DMF with 0.1 *M* TBAP as the supporting electrolyte. The cathodic scan showed two responses with E_f values of –0.7 V (ΔE_p = 270 mV) and –1.2 V (ΔE_p= 130 mV). The data agree well with those of other reported dioxovanadium(V) complexes[47,48].

Crystal structure of the complex

Complex **1** was characterized by single crystal X-ray diffraction method. It crystallizes in $P2_1/c$ space group of the monoclinic crystal system with four molecules in the unit cell and MeOH as the lattice solvent molecule. A perspective view of the complex is shown in Fig. 3. The molecular structure showed a discrete mononuclear penta-coordinated V^VNO_4 coordination geometry where vanadium atom is coordinated to the chelating O,N,O-donor vitamin-B6 Schiff base. It has a cis-oriented dioxovanadium(V) moiety. The V=O bond lengths are 1.6180(10) and 1.6571(9) Å. The V–O distances involving the phenolato moieties of the Schiff base are 1.9187(9) and 1.9356(9) Å. The V–N bond distance of 2.2138(11) Å is long due to *trans* effect of the V=O moiety. Selected bond lengths and angles data are presented in Table 2. The structure showed the presence of MeOH as the solvent of crystallization. The solid-state

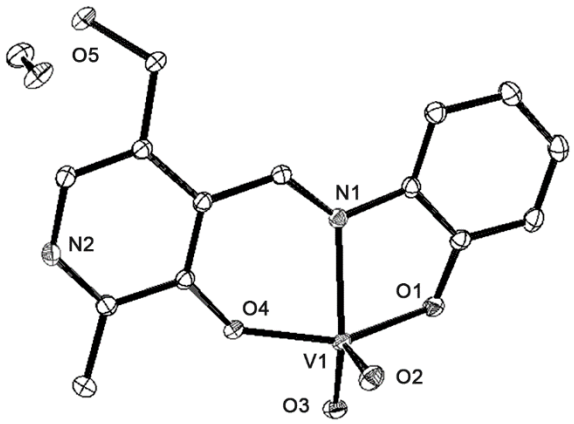

Fig. 3 — An ORTEP view of the complex is shown with the atom numbering for the metal and hetero atoms.

Table 2 – Selected bond distances (Å) and angles (°) for **1**·MeOH[a]

V(1)-O(2)	1.6180(10)
V(1)-O(3)	1.6571(9)
V(1)-O(4)	1.9187(9)
V(1)-O(1)	1.9356(9)
V(1)-N(1)	2.2138(11)
C(15)-H(17)	1.02(3)
O(2)-V(1)-O(3)	108.45(5)
O(2)-V(1)-O(4)	104.46(5)
O(3)-V(1)-O(4)	94.30(4)
O(2)-V(1)-O(1)	102.70(5)
O(3)-V(1)-O(1)	92.72(4)
O(4)-V(1)-O(1)	148.08(4)
O(2)-V(1)-N(1)	104.19(4)
O(3)-V(1)-N(1)	147.11(4)
O(4)-V(1)-N(1)	81.20(4)
O(1)-V(1)-N(1)	76.15(4)

[a] Estimated standard deviations (esd) in parenthesis.

structure of complex **1** shows chemically important hydrogen bonding interactions between the solvent and the complex. The molecules form dimeric stacked structure assisted with hydrogen-bonding interactions with the MeOH molecules (Fig. 4). The N-H protons of the pyridinium units also form interactions with the V=O bonds. This is also in support with the theoretical data obtained from the DFT calculations showing the presence of a positive surface potential on the pyridinium moiety and negative surface potential on the V=O bonds.

Theoretical studies

Geometry optimization calculations were performed using coordinates from the X-ray structure by B3LYP method and 6-31G(d) basis set for all the atoms to

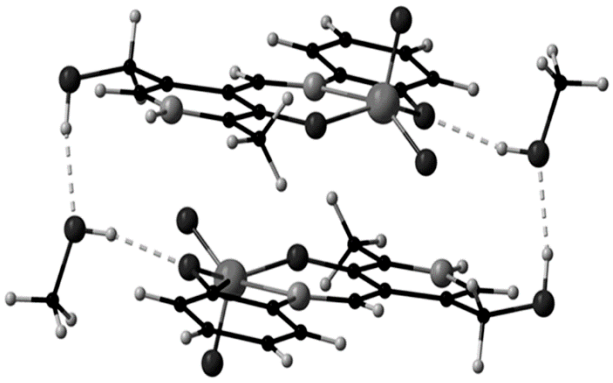

Fig. 4 — Intermolecular interaction between the complex and the solvent molecules.

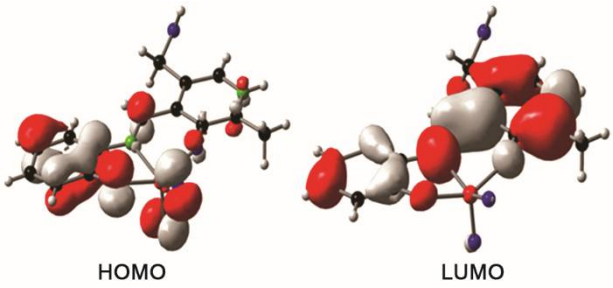

Fig. 5 — The frontier molecular orbitals of the complex.

understand the electronic structure of the complex[62-66]. The energy optimized structure of the complex showed that the vanadium(V) centre is coordinated to the chelating O,N,O-donor vitamin-B6 Schiff base and two oxo atoms giving a distorted square-pyramidal coordination geometry as observed in the crystal structure with similar bonding parameters. As shown in Fig. 5, the HOMO is located on the amino-phenolic moiety whereas the LUMO is located on the protonated aromatic part, i.e. the pyridiniumphenolate moiety which could facilitate charge-transfer upon electronic excitation of the molecule thus giving the possibility of having the PDT activity. The pyridinium moiety can be regarded as an electron acceptor unit whereas the amino-phenolic moiety is an electron rich system. This is evident from the electrostatic potential surface of the complex, shown in Fig. 6.

Photocytotoxicity

The ability of the complex to inhibit the cellular growth and induce cell death upon visible light-activation with 400-700 nm broad band light in human cervical cancer HeLa, breast cancer MCF-7 and normal fibroblast 3T3 cells was studied by MTT assay[67]. The choice of the excitation wavelength is based on the presence of a ligand→metal charge transfer (LMCT)

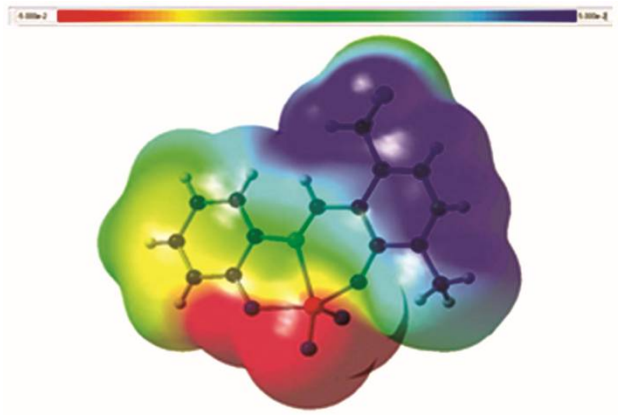

Fig. 6 — Electrostatic potential surface of the complex (isovalue = 0.004) as obtained from the DFT optimized geometry.

band near 460 nm in the electronic spectrum of the complex. The complex showed light induced reduction in the HeLa and MCF-7 cells viability in a dose-dependent manner giving the IC_{50} values of 15.6±1.2 μ*M* in HeLa and 18.8±1.4 μ*M* in MCF-7 cells, while being less toxic in the dark (IC_{50} > 75 μ*M*) even after 72 h of incubation (Fig. 7). The complex is less active against normal 3T3 cells compared to the cancer cells (IC_{50}: 65.7±2.8 μ*M* in light and >100 μ*M* in the dark for 3T3 cells). This could be due to lower cellular uptake of the complex in 3T3 normal cells considering the facts that (i) rapidly proliferating cancer cells have high demand for VB6 compared to the normal cells and (ii) the presence of high density of VB6 transporting membrane carrier (VTC) in cancer cells over the normal ones. The IC_{50} value of the complex upon light exposure increased to 56.4±3.6 μ*M* when it is pre-incubated with 4.0 mmol vitamin-B6. This suggests that uptake of this complex is mainly via VTC mediated diffusion pathway. The results are of importance considering tumour targeting potential and significant PDT activity of this complex compared to other known dioxovanadium(V) complexes[47,48].

DCFDA assay for ROS

Reactive oxygen species (ROS) plays a crucial role to generate oxidative stress in cells inducing cell apoptosis by the photoactive metal complexes[4,8,14]. Hence, 2',7'-dichlorofluorescein diacetate (DCFDA) assay was carried out to detect any photo-assisted generation of intracellular ROS in the presence of the complex. DCFDA is a non-fluorescent and cell permeable fluorogenic probe. Its cleavage by intracellular esterases and oxidation by ROS generates green fluorescent DCF with an emission maximum at ~525 nm which can be detected by

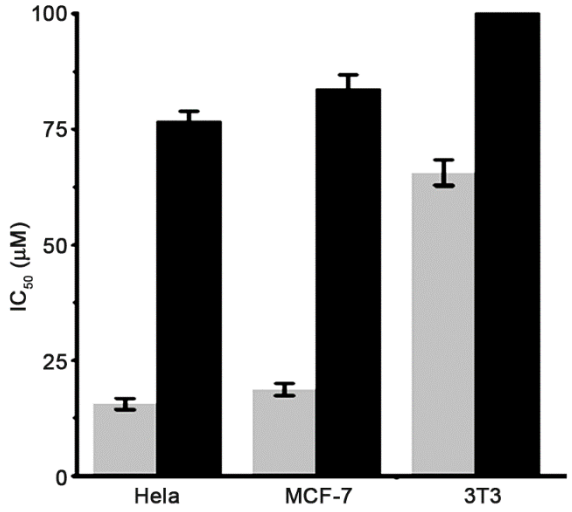

Fig. 7 — Photo-induced cytotoxicity of complex **1** in cervical HeLa, breast cancer MCF-7 and 3T3 normal cells on 4 h incubation in the dark (black bar) followed by photo-irradiation with visible light (400–700 nm, 10 *J* cm^{-2}) (grey bar).

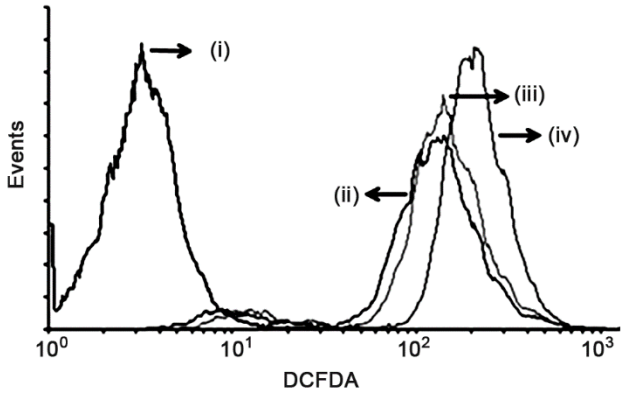

Fig. 8 — FACS analysis for ROS generation by complex **1** performed using DCFDA assay. Generation of ROS is highlighted by the shift in the fluorescence intensity in HeLa cells treated with the complex under different experimental conditions; (i) cells alone, (ii) cells+DCFDA, (iii) cells+ DCFDA+**1** (dark) and (iv) cells+DCFDA+1 (light).

FACS analysis[68]. HeLa cells treated with the complex and kept in dark did not show any generation of DCF. Whereas, a similar experiment in the presence of visible light (400–700 nm) showed significant shift of the emission band towards the right indicating ROS generation. This enhancement in the intensity of intracellular emission results from DCF formed from DCFDA on oxidation by ROS (Fig. 8). It can be inferred that the light triggered ROS generation induces oxidative cell stress resulting in the damage of nuclear DNA and cellular apoptosis.

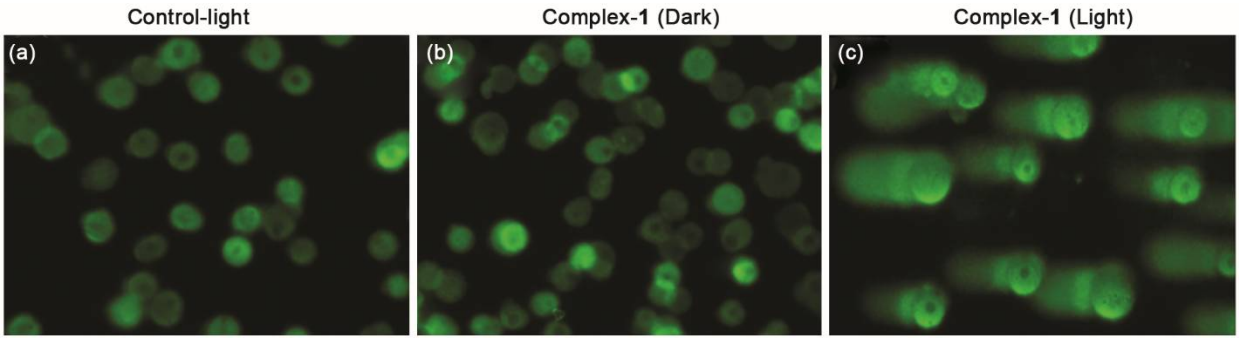

Fig. 9 — A representative image showing increase in the relative tail length by complex **1** upon photo-irradiation with visible light (400–700 nm) in the modified alkaline comet assay in HeLa cells. Panel (a) is the complex untreated control. Panel (b) shows the complex in darkness. Panel (c) is for the complex after photo-irradiation using visible light.

Annexin-V-FITC/PI assay with the green emitting fluorogenic probe that binds to phosphatidylserine was done to study the nature of cell death. Annexin-V is a calcium ion dependent phospholipid binding protein. Apoptosis mediated cell death results phosphatidylserine remaining in the inner leaflet of lipid bilayer in healthy cells and comes out at outer leaflet due to a change in the phospholipid asymmetry. This morphological change can be detected using Annexin-V-FITC probe. The red emitting nuclear staining propidium iodide dye was used as a secondary marker. Cells at early apoptotic stage can be identified as single positive population for annexin-V-FITC, while necrotic cell population can be stained by PI. The double positive cell population is assigned to the late apoptotic cells with compromised cell membrane. To examine the cellular apoptosis upon visible light irradiation, HeLa cells were treated with the complex (20 μ*M*, 4 h incubation) followed by photo-irradiation using visible light. Nearly 32% of the cells were found to be in an early apoptotic stage and ~10% of the cells were in a late apoptotic stage. Necrotic population was found to be significantly low suggesting an overall apoptotic mode of photo-induced cell death. The complex did not induce any significant cell death when kept in the dark.

Damage of nuclear DNA: Comet assay

Alkaline comet assay was used to visualize any damage of the nuclear DNA. This method is generally used to detect any DNA damage at the single cell level. Upon agarose gel electrophoresis, the damaged DNA showed formation of a tail, as the damaged DNA migrate faster compared to the undamaged DNA. When the complex was photo-activated in the HeLa cells and the DNA was analysed by alkaline comet assay, a significant increase in the tail length was observed compared to the complex untreated control or the dark control (Fig. 9). The Comet assay results suggest that single cell's DNA underwent degradation as a consequence of the visible light (400-700 nm) triggered apoptosis induced by the complex.

Conclusions

A new dioxovanadium(V) complex of vitamin-B6 Schiff base was prepared as a tumour targeting, visible light-induced photocytotoxic agent. The structurally characterized complex showed significant cell death in visible light (400-700 nm) targeting primarily the cancer cells, while being less toxic in the dark or in the 3T3 normal cells. The complex showed cellular internalization by VTC-mediated diffusion pathway. The complex on photo-activation induced cellular apoptosis by forming intracellular reactive oxygen species while remaining inactive under darkness as evidenced from the Annexin V-FITC/PI and DCFDA data. While oxovanadium(IV) complexes are known for their visible light-induced anticancer activity, dioxovanadium(V) complexes showing similar activity are virtually unknown in the chemistry of photodynamic therapy. The results are of significance considering the ability of the complex with a VO_2^+ moiety to act as potential DNA crosslinking agent on metal reduction and on photo-activation akin to those reported for the six-coordinated platinum(IV) prodrugs[69].

Supplementary Data

The crystallographic data have been deposited with the Cambridge Crystallographic Data Centre under CCDC reference number 1508677 for **1**·MeOH. The copies of this information may be obtained free of

charge from the Director, CCDC, 12 Union road, Cambridge, BC2 1EZ, UK; Fax: +44 1223 336 033, Email: deposit@ccdc-cam.ac.uk or www:http:// www.ccdc.cam.ac.uk.

Acknowledgement

We thank the Department of Science and Technology (DST), Government of India, for financial support (SR/S5/MBD-02/2007 and EMR/2015/000742). ARC thanks the DST for J C Bose national fellowship. SB and AK thank Indian Institute of Science (IISc), Bangalore, India, for fellowships.We are thankful to the Alexander von Humboldt Foundation for donation of an electrochemical system and Mr R N Samajdar for electrochemical data

References

1 Celli J P, Spring B Q, Rizvi I, Evans C L, Samoke K S, Verma S, Pogue B W & Hasan T, *Chem Rev*, 110 (2010) 2795.
2 Bonnett R, *Chemical Aspects of Photodynamic Therapy*, (Gordon & Breach, London, UK,) 2000.
3 Schatzschneider U, *Eur J Inorg Chem*, (2010), 1451.
4 Banerjee S & Chakravarty A R, *Acc Chem Res*, 48 (2015) 2075.
5 Chakravarty A R & Roy M, *Prog Inorg Chem*, 57 (2012) 119.
6 Smith N A & Sadler P J, *Phil Trans R Soc London, Ser A*, 371 (2013) 20120519.
7 Canelon I R & Sadler P J, *Inorg Chem*, 52 (2013) 12276.
8 Mari C, Pierroz V, Ferrarib S & Gasser G, *Chem Sci*, 6 (2015) 2660.
9 Banerjee S, Prasad P, Hussain A, Khan I, Kondaiah P & Chakravarty A R, *Chem Commun*, 48 (2012) 7702.
10 Banerjee S, Pant I, Khan I, Prasad P, Hussain A, Kondaiah P & Chakravarty A R, *Dalton Trans*, 44 (2015) 4108.
11 Banerjee S, Prasad P, Khan I, Hussain A, Kondaiah P & Chakravarty A R, *Z Anorg Allg Chem*, 640 (2014) 1195.
12 Kar M & Basak A, *Chem Rev*, 107 (2007) 2861.
13 Mao J, Zhang Y, Zhu J, Zhang C & Guo Z, *Chem Commun*, (2009) 908.
14 Chakrabarti M, Banik N L & Ray S K, *PLoSOne*, 8 (2013) e55652.
15 Robertson C A, Evans D H & Abrahamse H, *J Photochem Photobiol B: Biology*, 96 (2009) 1.
16 Marrachea S, Pathak R K & Dhar S, *Proc Natl Acad Sci USA*, 111 (2014) 10444.
17 Sarkar T, Banerjee S & Hussain A, *RSC Adv*, 5 (2015) 29276.
18 Sarkar T, Butcher R J, Banerjee S, Mukherjee S & Hussain A, *Inorg Chim Acta*, 439 (2016) 8.
19 Sarkar T, Banerjee S & Hussain A, *RSC Adv*, 5 (2015) 16641.
20 Banerjee S, Dixit A, Kumar A, Mukherjee S, Karande A A & Chakravarty A R, *Eur J Inorg Chem*, (2015) 3986.
21 Banerjee S, Dixit A, Karande A A & Chakravarty A R, *Eur J Inorg Chem*, (2015) 447.
22 Zhou W, Wang X, Hu M, Zhua C & Guo Z, *Chem Sci*, 5 (2014) 2761.
23 Bhattacharyya A, Dixit A, Mitra K, Banerjee S, Karande A A & Chakravarty A R, *Med Chem Commun*, 6 (2015) 846.
24 Garai A, Pant I, Banerjee S, Banik B, Kondaiah P & Chakravarty A R, *Inorg Chem*, 55 (2016) 6027.
25 Kumar A, Dixit A, Banerjee S, Bhattacharyya A, Garai A, Karande A A & ChakravartyA R, *Med Chem Commun*, 7 (2016) 1398.
26 Knoll J D & Turro C, *Coord Chem Rev*, 282−283 **(**2015) 110.
27 Chakraborty I, Carrington S J & Mascharak P K, *Acc Chem Res*, 47 (2014) 2603.
28 Renfrew A K, Bryce N S & Hambley T W, *Chem Eur J*, 21 (2015) 15224.
29 Renfrew A K, Bryce N S & Hambley T W, *Chem Sci*, 4 (2013) 3731.
30 Venkatesh V, Wedge C J, Canelón I R, Habtemariam A & Sadler P J, *Dalton Trans*, 45 (2016) 13034.
31 Mitra K, *Dalton Trans*, 45 (2016) 19157.
32 Ding S & Bierbach U, *Dalton Trans*, 45 (2016) 13104.
33 Ojima I, Zuniga E S, Berger W T & Seitz J D, *Future Med Chem*, 4 (2012) 33.
34 Chen S, Zhao X, Chen J, Chen J, Kuznetsova L, Wong S S & Ojima I, *Bioconjug Chem*, 21 (2010) 979.
35 Banerjee S, Dixit A, Shridharan R N, Karande A A & Chakravarty A R, *Chem Commun*, 50 (2014) 5590.
36 Banerjee S, Dixit A, Karande A A & Chakravarty A R, *Dalton Trans*, 45 (2016) 783.
37 Mukherjee N, Podder S, Banerjee S, Majumdar S, Nandi D & Chakravarty A R, *Eur J Med Chem*, 122 (2016) 497.
38 Combs G F, *The Vitamins: Fundamental Aspects in Nutrition and Health*, (Elsevier, San Diego), 2008.
39 Mooney S, Leuendorf J E, Hendrickson C & Hellmann H, *Molecules*, 14 (2009) 329.
40 Hellmann H & Mooney S, *Molecules*, 15 (2010) 442.
41 Zhang P, Suidasari S, Hasegawa T, Yanaka N & Kato N, *Oncology Rep*, 31 (2014) 2371.
42 Pandey S, Garg P, Lee S, Choung H W, Choung Y H, Choung P H & Chung J H, *Biomaterials*, 35 (2014) 9332.
43 Pandey S, Garg P, Lim K T, Kim J, Choung Y H, Choi Y J, Choung P H, Cho C S & Chung J H, *Biomaterials*, 34 (2013) 3716.
44 Clarke M J, Zhu F & Frasca D R, *Chem Rev*, 99 (1999) 2511.
45 Rehder D, Pessoa J C, Geraldes C F G C, Castro M M C A, Kabanos T, Kiss T, Meier B, Micera G, Pettersson L, Rangel M, Salifoglou A, Turel I & Wang D, *J Biol Inorg Chem*, 7 (2002) 384.
46 Crans D C & Tracey A S in *Vanadium Compounds:* Chemistry, Biochemistry, *and* Therapeutic Applications edited by A S Tracey, D C Crans, *(American Chemical Society, Washington,USA)* (1998) 2.
47 Dash S P, Panda A K, Pasayat S, Dinda R, Biswas A, Tiekink E R T, Mukhopadhyay S, Bhutia S K, Kaminskye W & Sinnf E, *RSC Adv*, 5 (2015) 51852.
48 Dash S P, Panda A K, Pasayat S, Majumder S, Biswas A, Kaminsky W, Mukhopadhyay S, Bhutia S K, & Dinda R, *J Inorg Biochem*, 144 (2015) 1.
49 Perrin D D, Armarego W L F & Perrin D R, *Purification of Laboratory Chemicals*, (Pergamon Press, Oxford), 1980.
50 Sharma D, Sahoo S K, Chaudhary S, Bera R K & Callan J F, *Analyst*, 138 (2013) 3646.

51 Walker N & Stuart D, *Acta Crystallogr*, A39 (1983) 158.
52 Sheldrick G M, *SHELX-97, Programs for Crystal Structure Solution and Refinement* (University of Göttingen, Göttingen, Germany) 1997.
53 Farrugia J L, *J Appl Crystallogr*, 32 (1999) 837.
54 Farrugia L J, *J Appl Crystallogr*, 45 (2012) 849.
55 Motulsky H J, *Prism 5 Statistics Guide*, (GraphPad Software Inc, San Diego, CA), 2007, [http://wwwgraphpadcom].
56 Takanashi T, Ogura Y, Taguchi H, Hashizoe M & Honda Y, *Invest Ophthalmol Vis Sci*, 38 (1997) 2721.
57 Soni C & Karande A A, *Mol Immunol*, 47 (2010) 2458.
58 Patra D, Biswas N, Kumari B, Das P, Sepay N, Chatterjee S, Drew M G B & Ghosh T, *RSC Adv*, 5 (2015) 92456.
59 Banerjee S, Hussain A, Prasad P, Khan I, Banik B, Kondaiah P & Chakravarty A R, *Eur J Inorg Chem*, (2012) 3899.
60 Geary W J *Coord Chem Rev*, 7 (1971) 81.
61 Ali I, Wani W A & Saleem K, *Synth React Inorg, Metal-Org Nano-Metal Chem*, 43 (2013) 1162.
62 Becke A D, *Phys Rev*, A38 (1998) 3098.
63 Becke A D, *J Chem Phys*, 98 (1993) 5648.
64 Lee C, Yang W & Parr R G, *Phys Rev, B* 37 (1988) 785.
65 Hay P J & Wadt W R, *J Chem Phys*, 82 (1985) 284.
66 *Gaussian 09, Revision A02*, (Gaussian, Inc, Wallingford CT), 2009.
67 Mosmann T, *J Immunol Methods*, 65 (1983) 55.
68 Keston A S & Brandt R, *Anal Biochem*, 11 (1965) 1.
69 Zhao Y, Woods J A, Farrer N J, Robinson K S, Pracharova J, Kasparkova J, Novakova O, Li H, Salassa L, Pizarro A M, Clarkson G J, Song L, Brabec V & Sadler P J, *Chem Eur J*, 19 (2013) 9578.

Arun Kumar and Samya Banerjee contributed equally.